

Communication

Asperversins A and B, Two Novel Meroterpenoids with an Unusual 5/6/6/6 Ring from the Marine-Derived Fungus *Aspergillus versicolor*

Huaqiang Li, Weiguang Sun, Mengyi Deng, Changxing Qi, Chunmei Chen, Hucheng Zhu, Zengwei Luo, Jianping Wang *, Yongbo Xue *  and Yonghui Zhang * 

Hubei Key Laboratory of Natural Medicinal Chemistry and Resource Evaluation, Tongji Medical College, Huazhong University of Science and Technology, Wuhan 430030, China; lihuaqiang2009@126.com (H.L.); weiguang_s@hust.edu.cn (W.S.); DengMengyi222@163.com (M.D.); kingqcx@sina.cn (C.Q.); chenchenmei@hust.edu.cn (C.C.); zhuhucheng@hust.edu.cn (H.Z.); luozengwei@hust.edu.cn (Z.L.)

* Correspondence: jpwang1001@163.com (J.W.); yongboxue@hust.edu.cn (Y.X.); zhangyh@mails.tjmu.edu.cn (Y.Z.); Tel.: +86-027-8369-2892 (Y.Z.)

Received: 17 April 2018; Accepted: 14 May 2018; Published: 23 May 2018



Abstract: Asperversins A (1) and B (2), two novel meroterpenoids featuring an uncommon 5/6/6/6 ring system, along with five new analogues (3–7) and a known compound asperdemin (8), were obtained from the marine-derived fungus *Aspergillus versicolor*. Their structures and absolute configurations were confirmed by extensive spectroscopic analyses, single-crystal X-ray diffraction studies, and electronic circular dichroism (ECD) calculation. All new compounds were tested for their acetylcholinesterase enzyme (AChE) inhibitory activities and cytotoxic activities, of which compound 7 displayed moderate inhibitory activity against the AChE with an IC₅₀ value of 13.6 μM.

Keywords: *Aspergillus versicolor*; meroterpenoids; asperversins; acetylcholinesterase enzyme

1. Introduction

Meroterpenoids are hybrid secondary metabolites that partially derive from the terpenoid pathways [1]. Naturally occurring meroterpenoids have been isolated from a variety of sources including animals, plants, bacteria, and fungi, [2] and are exemplified by ubiquinone-10 (coenzyme Q10) [3], α-tocopherol (vitamin E) [4], vinblastine [5], merochlorin A [6,7], and teleocidin B-4 [8].

Biosynthetically, the complex structures of fungal meroterpenoids are mostly derived from simple precursors like a linear isoprenoid or the C-2 carbon unit acetyl-CoA, via a series of chemical transformations catalyzed by two enzyme families, terpene cyclases and polyketide synthases (PKSs) [9,10]. In addition to the enormous structural diversity, fungal meroterpenoids have attracted wide interest from the scientific community due to their broad spectrum of pharmacological activities [11–14].

During our investigation of bioactive metabolites from fungi [15–19], many novel meroterpenoids were isolated from various fungi. Asperterpene A, obtained from *Aspergillus terreus*, represents a potential lead compound and a versatile scaffold for the development of drugs for the treatment of Alzheimer's disease [15]. Spiroaspertrione A, bearing a unique spiro[bicyclo[3.2.2]nonane-2,1'-cyclohexane] carbocyclic skeleton, shows an effective activity against methicillin-resistant *Staphylococcus aureus* (MRSA) [16]. The metabolites of the fungus *Aspergillus versicolor*, that were obtained from mud from the South China Sea, are reported here. This endeavor resulted in the isolation of seven undescribed meroterpenoids, called as asperversins A–G (1–7), and a structurally related known compound, asperdemin (8) [20]. Notably, asperversins A (1) and B (2) have a unique 5/6/6/6 ring system that features a tetrahydrofuran

ring. Herein, the isolation, structure elucidation, plausible biosynthetic pathway, and the biological evaluations of compounds 1–7 are presented.

2. Results and Discussion

Asperversin A (1), a white amorphous powder, was established to have a molecular formula of $C_{24}H_{32}O_8$ by HRESIMS ion at m/z 449.2173 ($[M + H]^+$, calcd. For $C_{24}H_{33}O_8$, 449.2175), indicating 9 degrees of unsaturation. The strong IR absorptions at 1741 and 1703 cm^{-1} suggested the presence of ester and unsaturated ester groups. The 1H NMR data (in methanol- d_4 , Table 1) displayed an olefinic proton at δ_H 5.91 (d, $J = 1.0$ Hz, H-15), a methoxy group at δ_H 3.70 (s, OMe-24) and six methyl groups at δ_H 2.20 (d, $J = 1.0$ Hz, H₃-17), 2.07 (s, H₃-23), 1.43 (H₃-18), 1.31 (H₃-19), 1.26 (H₃-20), and 1.18 (H₃-21). The ^{13}C and DEPT spectra revealed the presence of three carbonyl carbons (δ_C 173.6, 171.6, and 167.1) and two enol systems (δ_C 165.1, 162.2, 102.2, and 98.5), three quaternary sp^3 carbons (two oxygenated), four methines (two oxygenated), three methylene carbons, and seven methyl groups.

Comparison of the 1H and ^{13}C NMR data (Tables 1 and 2) of 1 with the known compound asperdemin (8) [20] revealed their close similarities, except for the presence of an additional methoxy group (δ_H 3.70, δ_C 52.3) and an acetoxy unit. Further analyses of the 1H - 1H COSY and HMBC spectra of 1 indicated that 1 shared the same B/C/D ring system as that of 8 (Figure 1). The key HMBC correlation from H-6 to C-22 (δ_C 171.6) indicated the acetoxy group at C-6. Furthermore, the 1H - 1H COSY cross-peaks of H-1/H₂-2 and the HMBC connections from H-1 to C-3, from H₂-2 to C-3, and from OMe to C-3 confirmed the existence of a methyl ester group in 1, rather than a seven-membered lactone. Although there was no obvious HMBC correlation to connect C-1 and C-4, the absence of hydroxyl at C-1 confirmed by the 1D and 2D NMR data in DMSO- d_6 and the chemical shifts of C-1 (δ_C 81.9 for 1; 68.0 for 8) and C-4 (δ_C 77.7 for 1; 84.8 for 8) indicated that C-1 and C-4 were connected with an ether bond to establish a tetrahydrofuran ring, which was consistent with the unsaturation degrees deduced by HRESIMS. Thus, the unusual tetrahydrofuran A ring replaced the seven-membered lactone ring, which distinguished compound 1 from other metabolites reported in this compound class.

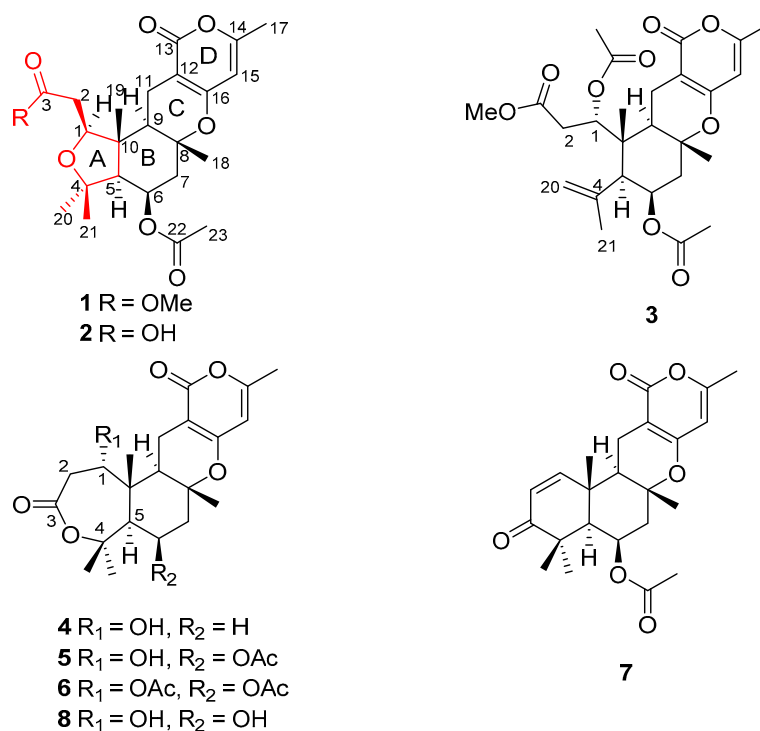


Figure 1. The structures of compounds 1–8.

The relative configuration of **1** was partially elucidated by the examination of its Nuclear Overhauser Effect Spectroscopy (NOESY) spectrum (Figure 2). The configuration of Me-19 was arbitrarily assigned as same as that of **8** in a β -orientation. Furthermore, the NOESY correlations of H₃-18/H-11b and H-11b/H₃-19 suggested their cofacial and β -orientation. In contrast, H-9 should be α -oriented. The NOESY correlations of H-1/H-9, H-9/H-5, and H-1/H-5 indicated their α -orientation. The spin-coupling constant ($J = 2.3$ Hz) of H-5 and H-6 suggested H-6 was equatorial. To confirmed the absolute configuration, the ECD calculation of **1** [1S,5S,6R,8R,9R,10R-1 (**1a**) and 1R,5R,6S,8S,9S,10S-1 (**1b**)] was conducted in MeOH using the time-dependent density functional theory (TD-DFT) method at the B3LYP/6-311+g (d, p) level. The experimental ECD of **1** matched well with the calculated ECD curve of **1a**, indicating the absolute configuration of **1** as 1S,5S,6R,8R,9R,10R (Figure 3).

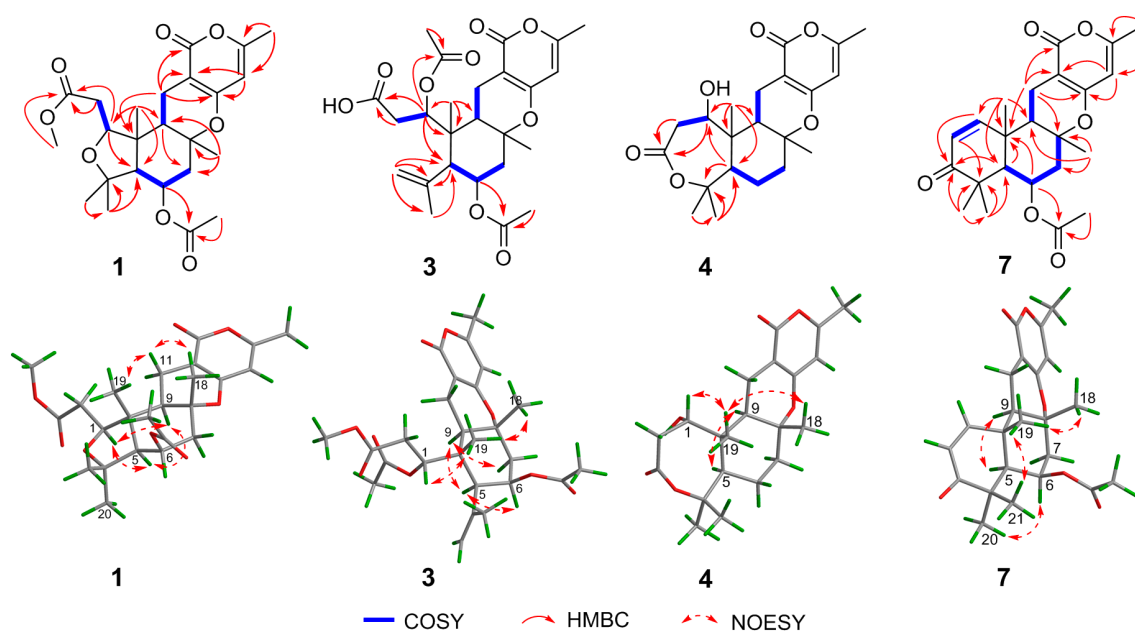


Figure 2. Key 2D correlations of compounds **1**, **3**, **4** and **7**.

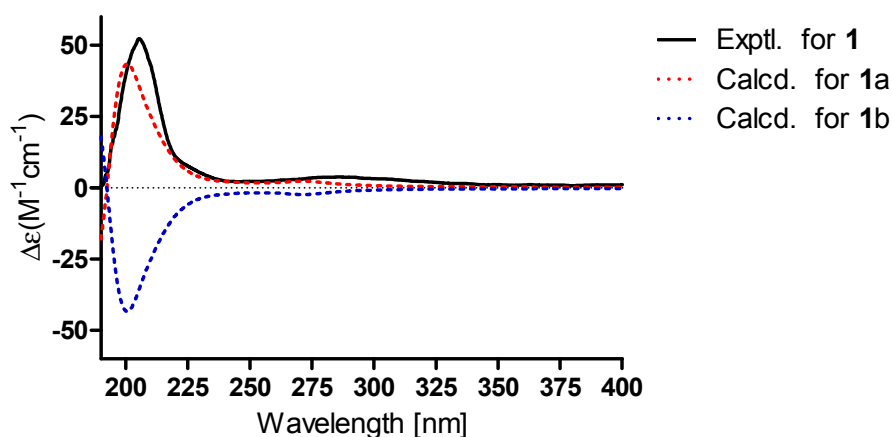


Figure 3. The experimental and calculated ECD of **1**.

Table 1. ¹H NMR Data for Compounds 1–7 (δ in ppm, *J* in Hz).

No.	1 ^a	2 ^a	3 ^a	4 ^b	5 ^b	6 ^a	7 ^a
1	3.98, dd (9.6, 2.3)	3.98, dd (9.7, 2.0)	5.42, dd (11.0, 1.8)	3.87, t (7.0)	3.79, dd (7.0, 5.2)	4.96, d (7.3)	7.08, d (10.2)
2	2.46, dd (15.7, 9.6) 2.68, m	2.39, m 2.63, dd (15.7, 2.0)	2.43, dd (14.8, 3.9) 2.88, dd (14.8, 1.8)	2.84, m 3.33, m	2.79, dd (16.0, 7.0) 3.32, d (16.0)	3.10, dd (16.2, 7.3) 3.55, d (16.2)	5.87, d (10.2)
5	2.13, d (2.3)	2.12, d (2.5)	2.49, d (3.0)	2.21, dd (12.1, 2.4)	2.38, d (2.3)	2.49, d (2.6)	1.98, d (1.8)
6	5.48, dd (4.5, 2.3)	5.48, m	5.27, m	1.67, m 1.92, m	5.52, dd (6.3, 3.0)	5.64, m	5.60, m
7	2.11, m 2.35, m	2.11, m 2.35, m	2.04, m 2.30, dd (14.4, 2.9)	1.72, m 2.06, m	1.92, dd, (14.6, 6.3) 2.26, dd, (14.6, 3.0)	2.05, m 2.40, dd (14.7, 3.0)	1.91, dd (14.7, 3.0) 2.42, m
9	1.97, dd (12.6, 5.2)	1.98, dd (11.3, 6.4)	1.90, dd (12.7, 4.6)	2.32, dd (12.5, 4.6)	2.34, m	2.15, m	1.81, dd (12.9, 4.3)
11	2.33, m 2.41, m	2.40, m 2.41, m	2.40, m 2.80, dd (17.4, 4.6)	2.08, m 2.43, dd (16.2, 4.6)	2.09, m 2.35, m	2.29, m 2.30, m	2.42, dd (16.5, 12.9) 2.76, dd (16.5, 4.3)
15	5.91, d (1.0)	5.92, d (1.1)	5.91, d (1.1)	5.81, d (1.1)	5.72, d (0.6)	5.91, d (1.1)	5.70, d (1.1)
17	2.20, d (1.0)	2.21, d (1.1)	2.21, d (1.1)	2.15, d (1.1)	2.05, d (0.6)	2.20, d (1.1)	2.18, d (1.1)
18	1.43, s	1.43, s	1.42, s	1.30, s	1.32, s	1.41, s	1.40, s
19	1.31, s	1.32, s	1.33, s	1.14, s	1.35, s	1.53, s	1.46, s
20	1.26, s	1.26, s	5.05, m 5.08, m	1.41, s	1.31, s	1.49, s	1.23, s
21	1.18, s	1.18, s	1.94, s	1.50, s	1.57, s	1.73, s	1.19, s
23	2.07, s	2.07, s	2.07, s		2.06, s	2.14, s	2.09, s
24	3.70, s		2.08, s				
25						1.99, s	

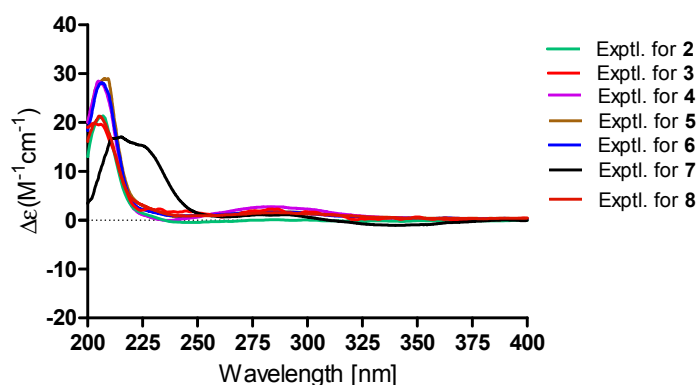
^a Recorded at 400 MHz in methanol-*d*₄; ^b recorded at 600 MHz in acetone-*d*₆.

Table 2. ^{13}C and DEPT NMR Data of Compounds 1–7 (δ in ppm, J in Hz).

No.	1 ^a	2 ^a	3 ^a	4 ^b	5 ^b	6 ^a	7 ^a
1	84.0, CH	84.5, CH	77.2, CH	68.8, CH	69.3, CH	72.6, CH	155.1, CH
2	37.3, CH ₂	37.9, CH ₂	36.2, CH ₂	39.8, CH ₂	39.9, CH ₂	36.3, CH ₂	125.1, CH
3	173.6, C	176.7, C	173.2, C	171.2, C	171.0, C	172.9, C	203.2, C
4	79.7, C	79.6, C	144.4, C	84.8, C	84.1, C	86.7, C	45.1, C
5	61.4, CH	61.5, CH	51.3, CH	50.2, CH	49.5, CH	51.3, CH	53.0, CH
6	68.3, CH	68.3, CH	73.4, CH	23.3, CH ₂	72.6, CH	72.7, CH	68.8, CH
7	45.3, CH ₂	45.3, CH ₂	43.3, CH ₂	40.6, CH ₂	43.3, CH ₂	43.3, CH ₂	43.4, CH ₂
8	81.5, C	81.6, C	81.2, C	80.9, C	79.9, C	80.4, C	79.3, C
9	48.1, CH	48.1, CH	44.2, CH	44.8, CH	44.4, CH	45.1, CH	46.9, CH
10	46.5, C	46.4, C	45.6, C	45.3, C	45.4, C	45.1, C	39.4, C
11	19.4, CH ₂	19.4, CH ₂	19.7, CH ₂	17.5, CH ₂	17.2, CH ₂	17.6, CH ₂	16.9, CH ₂
12	98.5, C	98.6, C	99.0, C	98.2, C	98.3, C	98.3, C	97.3, C
13	167.1, C	167.2, C	167.1, C	164.5, C	164.5, C	164.6, C	164.8, C
14	162.2, C	162.2, C	162.2, C	160.8, C	161.0, C	162.3, C	160.5, C
15	102.2, CH	102.0, CH	101.8, CH	100.6, CH	100.6, CH	101.7, CH	100.3, CH
16	165.1, C	165.2, C	164.8, C	163.3, C	162.8, C	166.8, C	162.7, C
17	19.5, CH ₃	19.5, CH ₃	19.5, CH ₃	19.5, CH ₃	19.5, CH ₃	19.5, CH ₃	19.7, CH ₃
18	23.0, CH ₃	23.0, CH ₃	22.1, CH ₃	20.9, CH ₃	21.9, CH ₃	22.0, CH ₃	22.0, CH ₃
19	12.4, CH ₃	12.5, CH ₃	15.3, CH ₃	15.2, CH ₃	16.2, CH ₃	16.0, CH ₃	18.1, CH ₃
20	30.5, CH ₃	30.6, CH ₃	117.7, CH ₂	34.9, CH ₃	33.9, CH ₃	33.9, CH ₃	26.6, CH ₃
21	25.5, CH ₃	25.6, CH ₃	26.5, CH ₃	24.0, CH ₃	26.4, CH ₃	26.2, CH ₃	22.8, CH ₃
22	171.6, C	171.7, C	171.5, C		170.2, C	171.2, C	169.7, C
23	21.3, CH ₃	21.3, CH ₃	20.9, CH ₃		21.4, CH ₃	21.3, CH ₃	21.5, CH ₃
24	52.3, OCH ₃		172.2, C			171.1, C	
25			21.4, CH ₃			20.6, CH ₃	

^a Recorded at 100 MHz in methanol-*d*₄; ^b recorded at 150 MHz in acetone-*d*₆.

The HRESIMS spectrum suggested a molecular formula of C₂₃H₃₀O₈ for compound **2**, indicating a molecular weight of 14 mass units lower than **1**. The ¹H and ¹³C NMR data of **2** (Tables 1 and 2) closely resembled those of compound **1**, except for the difference of chemical shift of carbonyl (C-3: δ_{C} 176.7 for **2**; 173.6 for **1**), and the absence of the methoxy group. Compound **2** was speculated to be the carboxylic acid analogue of **1**. The structure of **2** was confirmed by extensive analyses of its ¹H–¹H COSY and HMBC spectra. Compound **2** was confirmed to have the same relative and absolute configurations as **1** by the NOESY spectra and their similar ECD curves (Figures 1, 3 and 4).

**Figure 4.** The experimental ECD of 2–8.

Asperversin C (**3**), a white amorphous powder, has a molecular formula of C₂₆H₃₄O₉, which was determined on the basis of the HRESIMS ion peak at m/z 491.2269 ($[\text{M} + \text{H}]^+$, calcd. For C₂₆H₃₅O₉, 491.2281). The similar IR, UV, 1D, and 2D NMR spectra of **3** and **1** suggested both compounds shared the same B/C/D rings. A comparison of their 1D and 2D NMR data indicated the presence

of a double bond (δ_{H} 5.05 and 5.08, δ_{C} 117.7, CH₂-20; δ_{C} 144.4, C-4) and the absence of a methyl group in compound **3**. The location of the double bond between C-4 and C-20 was confirmed by the HMBC correlations from H₂-20 to C-4, C-5, and C-21, and from H₃-21 to C-4 and C-20. Moreover, the HMBC correlations from H-1 to C-24 and H₃-25 to C-24 defined the location of an additional acetoxy unit at C-1. Finally, the planar structure of **3** with the A ring opened was confirmed as shown (Figure 1). The NOE correlations from H-1/H₃-19, H₃-18/H₃-19 suggested H-1, Me-18, and Me-19 were β -oriented. In contrary, H-5, H-6 and H-9 were α -oriented based on the correlations of H-5/H-6 and H-5/H-9. In consideration of the similar specific rotation and ECD spectra (Figure 4), the absolute configuration of **3** was assigned as 1*R*,5*S*,6*R*,8*R*,9*R*,10*R*.

Asperversin D (**4**) possesses a molecular formula of C₂₁H₂₈O₆ with 16 units less than that of compound **8** on the basis of HRESIMS data. Comparison of the ¹H and ¹³C NMR data of **4** with those of **8** revealed the presence of an additional methylene group and the absence of an oxygenated methine group in **4**. Inspection of the 2D NMR of **4** indicated this methylene group (δ_{C} 23.3; δ_{H} 1.67 and 1.92) should be assigned to C-6 by the ¹H-¹H COSY correlations of H-5/H₂-6/H-7. The gross structure of **4** and its relative configuration were then confirmed by comprehensive analyses of the ¹H-¹H COSY, HMBC, and NOESY spectra. Finally, the absolute configuration of **4** was ascertained as 1*R*,5*S*,8*R*,9*R*,10*R* by a similar ECD spectrum to that of **1** (Figure 4).

Asperversin E (**5**), colorless crystals, exhibits a molecular formula of C₂₃H₃₀O₈ with nine degrees of unsaturation from a HRESIMS ion peak at *m/z* 457.1830 ([M + Na]⁺, calcd. For 457.1838). Close similarities were observed in the ¹³C NMR data (Table 2) between compounds **5** and **4**. Inspection of the 1D NMR spectra, HSQC, and HMBC spectra revealed that **5** contained an additional acetoxy group (δ_{H} 2.06, δ_{C} 21.4, and 170.2). Detailed HMBC correlations from H₃-23 (δ_{H} 2.06) to C-22 (δ_{C} 170.2) and from H-6 (δ_{H} 5.52) to C-22 confirmed the location. The X-ray crystallographic diffraction (Figure 5) revealed the configuration of **5** was 1*R*,5*S*,6*R*,8*R*,9*R*,10*R*.

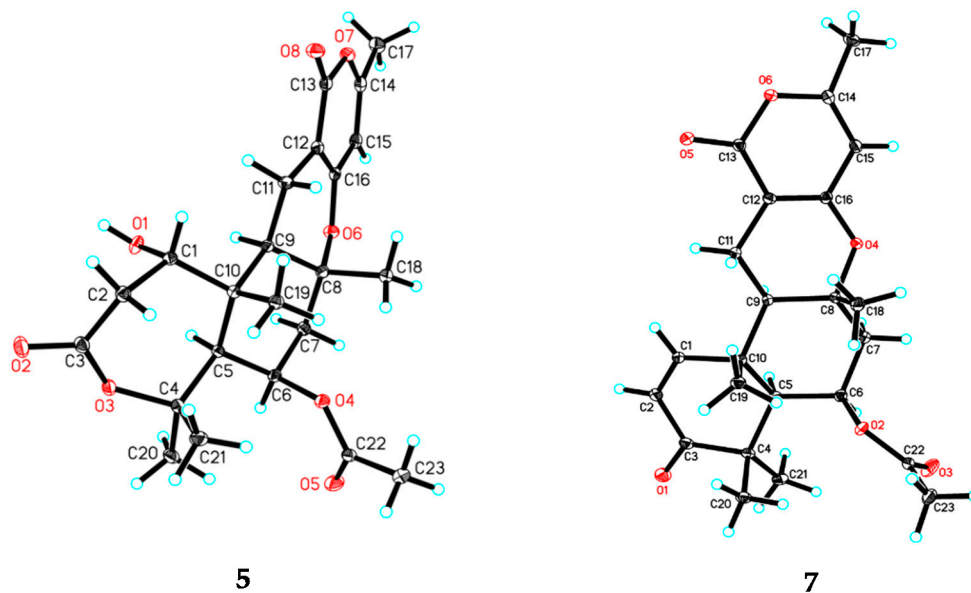


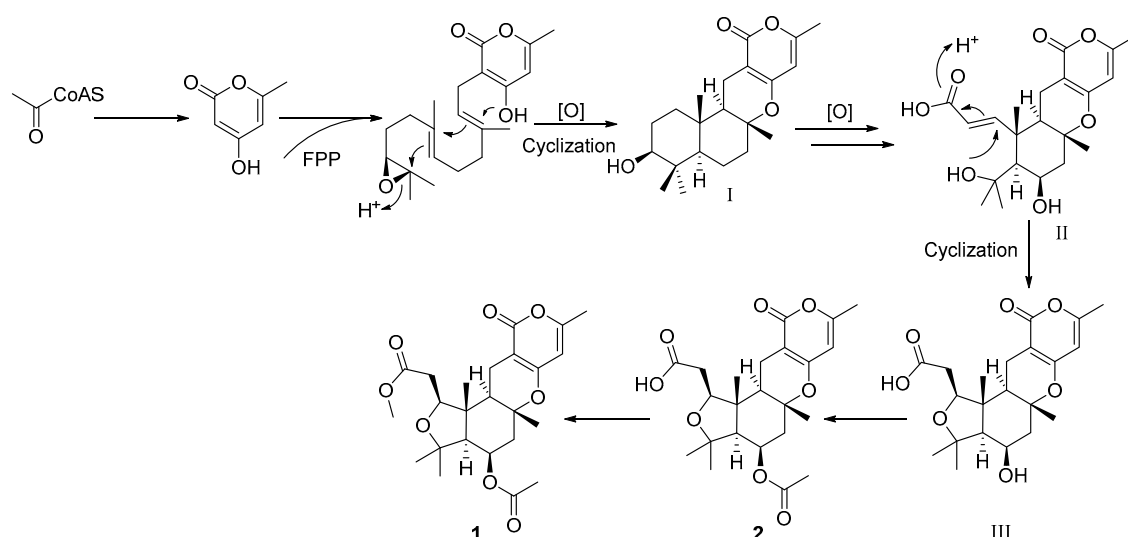
Figure 5. ORTEP drawings of compounds **5** and **7**.

A protonated molecular ion peak at *m/z* 477.2098 ([M + H]⁺, calcd. 477.2125) was obtained from the HRESIMS experiment and indicated asperversin F (**6**) has the molecular formula C₂₅H₃₂O₉. The ¹H and ¹³C NMR spectra of **6** showed there were two more acetoxy groups (δ_{H} 2.14, δ_{C} 21.3, and 171.2; δ_{H} 1.99, δ_{C} 20.6, and 171.1) than **4**. The locations of two acetoxy groups were assigned to C-1 and C-6 by the HMBC correlations from H-1 (δ_{H} 4.96) to C-24 and from H-6 (δ_{H} 5.64) to C-22, respectively. The relative

configuration and absolute configuration of **6** were determined by analyzing the NOESY spectrum and by comparing its ECD spectrum with that of **5** (Figure 4).

Asperversin G (**7**), colorless cubic crystals, has a molecular formula of $C_{23}H_{28}O_6$ based on the HRESIMS spectrum. The 1H and ^{13}C NMR data (Tables 1 and 2) of **7** resembled those of **5**, with the main difference being the presence of an α,β -unsaturated ketone group (δ_H 7.08, d, $J = 10.2$ Hz and 5.87, d, $J = 10.2$ Hz; δ_C 203.2, 155.1, and 125.1). The α,β -unsaturated ketone further constructed an 2-cyclohexen-1-one (ring A), as ascertained by the HMBC correlations from H_3 -19 to C-1, C-5, C-9, and C-10, from H-1 to C-3, from H-2 to C-3 and C-4, and from H_3 -20 and H_3 -21 to C-3, C-4, and C-5. The remainder of **7** was identical to **5** as elucidated by 2D NMR spectra. The absolute configuration of **7** was established unambiguously as 5*S*,6*R*,8*R*,9*R*,10*R* by a single-crystal X-ray diffraction (Figure 5).

Asperversins A (**1**) and B (**2**) were found to be the first examples of pyrone meroterpenoids featuring an exclusive 5/6/6/6 ring system compared to all known meroterpenoids [2]. Therefore, a plausible biosynthetic pathway is proposed to illustrate the generation of **1** and **2** (Scheme 1). Asperversins A (**1**) and B (**2**) are probably biosynthesized via a polyketide and mevalonate hybrid biogenetic pathway [2,21,22]. After a series of oxidations, the A ring of **I** was opened, and then, followed by the key electrophilic addition of OH-4 with the α,β -unsaturated carboxylic acid bond, the intermediate **III**, featuring a tetrahydrofuran ring, was derived from **II**. Compounds **2** and **1** were produced subsequently by an additional acetylation and methylation.



Scheme 1. Postulated biosynthetic pathway of compounds **1** and **2**.

All compounds (**1–8**) were inactive for cytotoxicity against A549, MCF-7, HepG2, and HL-60 cells, and did not have any antimicrobial effects against methicillin-resistant *Staphylococcus aureus* (MRSA), methicillin-sensitive *Staphylococcus aureus* (MSSA), *Escherichia coli*, or *Pseudomonas aeruginosa*. The acetylcholinesterase (AChE) inhibition effects of these compounds (**1–8**) were assessed by Ellman's spectrophotometric method [23] using human recombinant AChE with galanthamine as control compound (Table 3). Compound **7** exhibited the strongest inhibition to AChE with an IC_{50} value of 13.6 μM , and compounds **1–6** and **8** showed no activities up to a concentration of 40 μM .

The molecular docking studies were conducted in order to get an insight into the binding pattern and extent of binding of compound **7** with the target enzyme (Figure 6). This was mainly attributed to the basic skeleton of compound **7** which provided better binding prospects with the formation of hydrogen bonding interactions to the amino acid residues Glu 291 and Tyr 341 of the protein. So we speculated the α,β -unsaturated ketone group was the key pharmacophore for the acetylcholinesterase (AChE) inhibition effect.

Table 3. The inhibitory value and docking score of compounds 1–8 with AChE.

Compounds	Inhibitory Ratio at 100 μM	IC ₅₀ Value (μM) ^a	Docking Score ^b
1	35.7%	>40	3.25
2	36.2%	>40	3.89
3	27.6%	>40	2.76
4	50.2%	>40	5.32
5	48.7%	>40	4.98
6	62.9%	>40	5.87
7	92.4%	13.6	7.85
8	25.3%	>40	2.58
Galanthamine		3.57	

^a IC₅₀ value of compounds against AChE (μM); ^b Docking score/interaction potential of compounds with target protein.

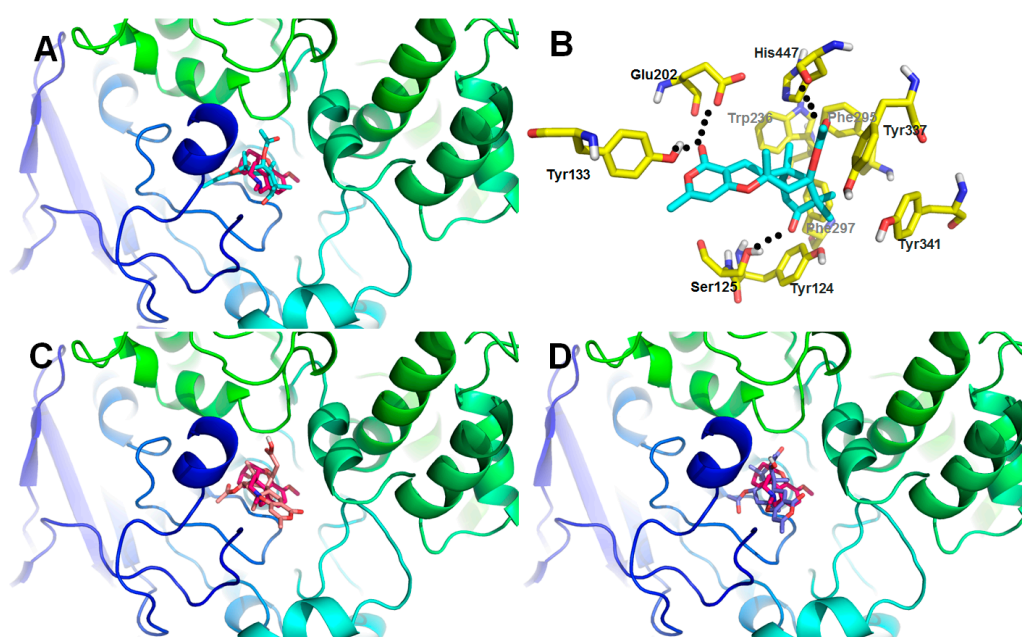


Figure 6. Low-energy binding conformations of compounds bound to AChE generated by virtual ligand docking. (A) Compound 7 was observed to occupy the active site with significant scores and adopted a conformation similar to that of galanthamine. (B) Compound 7 had the ability to form key hydrogen bonding interaction with residues Ser125, Tyr133, Glu202, and His447. (C,D) Compounds 2 (C) and 5 (D) were observed to occupy the active site with pretty low scores comparing with that of galanthamine.

3. Experimental Section

3.1. General Experimental Procedures

The NMR spectra were recorded on Bruker AM-400 and 600 spectrometers (Bruker, Karlsruhe, Germany). The ¹H and ¹³C NMR chemical shifts were referenced to the solvent or solvent impurity peaks for methanol-*d*₄ (δ_{H} 3.31 and δ_{C} 49.0), and acetone-*d*₆ (δ_{H} 2.05 and δ_{C} 206.3 and 29.8). The FT-IR spectra were determined with a Bruker Vertex 70 instrument (Bruker, Karlsruhe, Germany). The UV and ECD spectra were measured using a Perkin Elmer Lambda 35 UV spectrophotometer (PerkinElmer, Inc., Fremont, CA, USA) and a JASCO-810 ECD spectrometer (JASCO Co., Ltd., Tokyo, Japan), respectively. Optical rotations were measured by an AUTOPOL IV-T Automatic polarimeter (Rudolph Research Analytical, Hackettstown, NJ, USA).

HRESIMS data were obtained in the positive ion mode on a Thermo Fisher LTQ XL spectrometer (Thermo Fisher, Palo Alto, CA, USA). Crystal X-ray diffraction data were measured on a Rigaku XtaLAB PRO MM007HF (Rigaku, Tokyo, Japan). Semipreparative HPLC was carried out using an Agilent 1200 quaternary system with a UV detector using a reversed-phase C₁₈ column (5 μM, 10 × 250 mm, Welch Ultimate XB-C18). Column chromatography (CC) was performed using silica gel (100–200 and 200–300 mesh; Qingdao Marine Chemical Inc., Qingdao, China), ODS (50 μM, YMC, Kyoto, Japan), and Sephadex LH-20 (GE Healthcare Bio-Sciences AB, Uppsala, Sweden). Thin-layer chromatography (TLC) was performed on silica gel 60 F254 (Yantai Chemical Industry Research Institute, Yantai, China).

3.2. Fungi Material

The fungus *Aspergillus versicolor* was isolated from mud of the South China Sea. The sequence data for this strain have been submitted to DDBJ/EMBL/GenBank under accession no. 2081031. A voucher sample has been deposited in the culture collection of Tongji Medical College, Huazhong University of Science and Technology, P. R. China.

3.3. Fermentation and Extraction

The *Aspergillus versicolor* strain was cultured on potato dextrose agar (PDA) at 28 °C for 7 days to prepare the seed culture and inoculated into 100 sterilized Erlenmeyer flasks (1 L), which contained 200.0 g of rice and 160.0 mL of distilled water, then incubated at 28 °C for 28 days. Following incubation, the rice was soaked with 95% EtOH many times until the solvent was near-colorless at room temperature. Finally, solvent removal afforded a brown extract that was suspended in water (2 L) and extracted with EtOAc (1:1, *v/v*) three times. After removal of EtOAc, a dark brown gum (170 g) was obtained.

3.4. Isolation

The extracts (170.0 g) were subjected to a silica gel chromatography column (CC) eluting with PE/ EtOAc (20:1–0:1) progressively to obtain six fractions (Fr. 1–Fr. 6). Fr.3 was further separated with silica gel CC to yield four subfractions (Fr. 3.1–Fr. 3.4). The subfraction Fr. 3.1 was subjected to a Sephadex LH-20 (MeOH) to afford three parts (Fr. 3.1a–Fr. 3.1c). After crude purification of Fr. 3.1a by ODS column (MeOH–H₂O, 20:80–70:30, *v/v*), the second part of Fr. 3.1a (Fr. 3.1a-2, MeOH–H₂O, 60:40, *v/v*) was purified by repeated semi-preparative HPLC (MeCN–H₂O, 55:45, 2 mL/min) to yield **1** (9.3 mg, *t*_R 25.2 min), **2** (6.2 mg, *t*_R 28.5 min), **7** (23.6 mg, *t*_R 30.1 min).

Three subfractions (Frs. 3.2a–3.2c) were obtained from Fr. 3.2 by chromatography on an ODS column (MeOH–H₂O, 20:80–70:30, *v/v*). Fr.3.2b was chromatographed on ODS (MeOH–H₂O, 40:60–70:30) to afford a mixture (**4**, **5**, **6**, **8**) in 40% yield. The mixture was purified by semi-preparative HPLC (MeCN–H₂O, 40:60–60:40, 2 mL/min) to yield **8** (16.3 mg, *t*_R 25.5 min, 45:55), **5** (200.0 mg, *t*_R 27.2 min, 45:55), **4** (3.7 mg, *t*_R 21.0 min, 40:60), and **6** (10.2 mg, *t*_R 21.0 min, 40:60). Fr. 3.2c was chromatographed on ODS (MeOH–H₂O, 30:70–80:20, *v/v*) to yield four parts. Fr. 3.2c-2 (the second part of Fr. 3.2c, MeOH–H₂O, 50:50–60:40, *v/v*) was purified by repeated semi-preparative HPLC (MeCN–H₂O, 46:54, 2 mL/min) to yield **3** (2.78 mg, *t*_R 15.1 min).

3.4.1. Asperversin A (**1**)

C₂₄H₃₂O₈; a white amorphous powder; [α]_D²⁵ +46.7 (*c* 0.34, MeOH); UV (MeOH) λ_{\max} (log ϵ) 205 (4.51) and 286 (3.84) nm; IR (KBr) ν_{\max} 3445, 2958, 1741, 1710, 1654, 1588, 1444, 1403, 1384, 1237, 1194, 996 cm⁻¹; ECD (MeOH) λ_{\max} ($\Delta\epsilon$) = 205 (+25.02) and 286 (+1.86) nm; For ¹H NMR (400 MHz) and ¹³C NMR (100 MHz) data, see Tables 1 and 2; HRESIMS 449.2173 ([M + H]⁺, calcd. For C₂₄H₃₃O₈, 449.2175).

3.4.2. Aspersversin B (2)

$C_{23}H_{30}O_8$; a white amorphous powder; $[\alpha]^{25}_D +100.3$ (c 0.29, MeOH); UV (MeOH) λ_{max} ($\log \epsilon$) 202 (4.78) and 285 (4.14) nm; IR (KBr) ν_{max} 3433, 2963, 2929, 1740, 1710, 1652, 1584, 1446, 1407, 1235, 1194, 1028 cm^{-1} ; ECD (MeOH) λ_{max} ($\Delta\epsilon$) = 207 (+21.37) and 286 (+0.11) nm; For 1H NMR (400 MHz) and ^{13}C NMR (100 MHz) data, see Tables 1 and 2; HRESIMS m/z 457.1846 ($[M + Na]^+$, calcd. For $C_{23}H_{30}NaO_8$, 457.1838).

3.4.3. Aspersversin C (3)

$C_{25}H_{32}O_9$; a white amorphous powder; $[\alpha]^{25}_D +100.9$ (c 0.23, MeOH); UV (MeOH) λ_{max} ($\log \epsilon$) 205 (4.51) and 284 (3.87) nm; IR (KBr) ν_{max} 3425, 2922, 1743, 1711, 1655, 1591, 1233, 1192, 1032 cm^{-1} ; ECD (MeOH) λ_{max} ($\Delta\epsilon$) = 203 (+19.88) and 286 (+2.34) nm; For 1H NMR (400 MHz) and ^{13}C NMR (100 MHz) data, see Tables 1 and 2; HRESIMS m/z 491.2269 ($[M + H]^+$, calcd. For $C_{26}H_{35}O_9$, 491.2281).

3.4.4. Aspersversin D (4)

$C_{21}H_{28}O_6$; a white amorphous powder; $[\alpha]^{25}_D +98.4$ (c 0.25, MeOH); UV (MeOH) λ_{max} ($\log \epsilon$) 205 (4.77) and 286 (3.93) nm; IR (KBr) ν_{max} 3429, 2928, 1702, 1653, 1586, 1449, 1408, 1386, 1313, 1274, 1154, 1113 cm^{-1} ; ECD (MeOH) λ_{max} ($\Delta\epsilon$) = 205 (+23.13) and 285 (+2.24) nm; For 1H NMR (600 MHz) and ^{13}C NMR (150 MHz) data, see Tables 1 and 2; HRESIMS 377.1919 ($[M + H]^+$, calcd. For $C_{22}H_{29}O_8$, 377.1964).

3.4.5. Aspersversin E (5)

$C_{23}H_{30}O_8$; colorless crystals; $[\alpha]^{25}_D +75.5$ (c 0.20, MeOH); UV (MeOH) λ_{max} ($\log \epsilon$) 205 (4.57) and 286 (3.89) nm; IR (KBr) ν_{max} 3431, 2988, 2931, 1714, 1653, 1588, 1447, 1402, 1233, 1128, 1086 cm^{-1} ; ECD (MeOH) λ_{max} ($\Delta\epsilon$) = 208 (+28.96) and 281 (+1.86) nm; For 1H NMR (600 MHz) and ^{13}C NMR (150 MHz) data, see Tables 1 and 2; HRESIMS 457.1830 ($[M + Na]^+$, calcd. For $C_{23}H_{30}O_8Na$, 457.1838).

3.4.6. Aspersversin F (6)

$C_{25}H_{32}O_9$; a white amorphous powder; $[\alpha]^{25}_D +100.6$ (c 0.48, MeOH); UV (MeOH) λ_{max} ($\log \epsilon$) 205 (4.61) and 286 (3.77) nm; IR (KBr) ν_{max} 3462, 2992, 2934, 1736, 1655, 1590, 1448, 1409, 1374, 1230, 1202, 1131, 1024 cm^{-1} ; ECD (MeOH) λ_{max} ($\Delta\epsilon$) = 215 (+23.68) and 282 (+0.34) nm; For 1H NMR (400 MHz) and ^{13}C NMR (100 MHz) data, see Tables 1 and 2; HRESIMS 477.2143 ($[M + H]^+$, calcd. For $C_{25}H_{33}O_9$, 477.2098).

3.4.7. Aspersversin G (7)

$C_{23}H_{28}O_6$; colorless cubic crystals; $[\alpha]^{25}_D +110.2$ (c 0.21, MeOH); UV (MeOH) λ_{max} ($\log \epsilon$) 205 (4.60), 228 (4.18) and 285 (3.88) nm; IR (KBr) ν_{max} 3434, 2975, 2927, 2862, 1793, 1706, 1674, 1587, 1448, 1408, 1257, 1232, 1141 cm^{-1} ; ECD (MeOH) λ_{max} ($\Delta\epsilon$) = 215 (+16.60), 291 (+1.11) and 342 (−1.01) nm; For 1H NMR (400 MHz) and ^{13}C NMR (100 MHz) data, see Tables 1 and 2; HRESIMS $[M + H]^+$ m/z 401.1977 (calcd. For $C_{23}H_{29}O_6$, 401.1964).

3.5. X-ray Crystal Structure Analysis

The crystallographic data for **5** (deposition no. CCDC 1816743), and **7** (deposition no. CCDC 1813401) have been deposited in the Cambridge Crystallographic Data Centre. Copies of the data can be obtained free of charge from the Cambridge Crystallographic Data Centre.

3.5.1. Crystal Data for Aspersversin E (5)

$C_{23}H_{30}O_8 \cdot H_2O$ ($M = 452.48$ g/mol), orthorhombic, space group $P2_12_12_1$ (no. 19), $a = 9.95215(4)$ Å, $b = 12.89469(4)$ Å, $c = 17.07108(6)$ Å, $V = 2190.729(13)$ Å³, $Z = 4$, $T = 100.01(10)$ K, μ (CuK α) = 0.881 mm^{−1}, $D_{calc} = 1.372$ g/cm³, 23,143 reflections measured ($8.594 \leq 2\theta \leq 147.672$), 4396 unique ($R_{int} = 0.0181$, $R_{sigma} = 0.0097$) which were used in all calculations. The final R_1 was 0.0274 ($I > 2\sigma(I)$) and wR_2 was 0.0772. The Flack parameter was 0.039(16).

3.5.2. Crystal Data for Asperversin G (7)

$C_{23}H_{28}O_6$ ($M = 400.45$ g/mol), monoclinic, space group $P2_1$, $a = 8.77354(16)$ Å, $b = 13.09891(17)$ Å, $c = 9.64200(17)$ Å, $\alpha = 90.0^\circ$, $\beta = 116.686(2)^\circ$, $\gamma = 90.0^\circ$, $V = 990.06(3)$ Å³, $Z = 2$, $T = 100.01(10)$ K, μ (CuK α) = 0.790 mm⁻¹, $D_{calc} = 1.541$ g/cm³, 23,143 reflections measured ($10.268 \leq 2\theta \leq 147.12$), 3462 unique ($R_{int} = 0.0195$, $R_{sigma} = 0.0162$) which were used in all calculations. The final R_1 was 0.0276 ($I > 2\sigma(I)$) and wR_2 was 0.0738. The Flack parameter was 0.11(7).

3.6. Computational Methods

Monte Carlo conformational searches were carried out by the Spartan's 10 software using the Merck Molecular Force Field (MMFF). The conformers with a Boltzmann-population of over 5% were chosen for ECD calculations, and then the conformers were initially optimized at B3LYP/6-31+g (d, p) level in MeOH using the CPCM polarizable conductor calculation model. The theoretical calculation of ECD was conducted in MeOH using Time-dependent Density functional theory (TD-DFT) at the B3LYP/6-311+g (d, p) level for all conformers of compounds **1a** and **1b**. Rotatory strengths for a total of 50 excited states were calculated. ECD spectra were generated using the program SpecDis 1.6 (University of Würzburg, Würzburg, Germany) and GraphPad Prism 5 (University of California San Diego, USA) from dipole-length rotational strengths by applying Gaussian band shapes with $\sigma = 0.3$ eV [24].

3.7. Acetylcholinesterase Inhibitory Activities Assay

The inhibitory activities of compounds **1–8** against AChE were evaluated by Ellman's method with slight modification [25]. Briefly, 20 μ L AChE (0.05 U/mL) and 20 μ L different concentrations of compounds (0.1 M phosphate buffer, pH 8.0) containing 0.1% Triton X-100) were pre-incubated at 37 °C for 30 min, then 160 μ L of the assay solution which consisted of a 0.1 M phosphate buffer pH 8.0, with the addition of 600 μ M 5,5'-dithio-bis (2-nitrobenzoic acid) and 550 μ M acetylthiocholine iodide (ATCh) were added in the 96-well plates. The absorbance value at 425 nm was recorded for 15 min and enzyme activity was calculated from the slope of the obtained linear trend. The reaction rates were compared and the % inhibition due to the presence of tested inhibitors was calculated. Each concentration was analyzed in triplicate, and IC_{50} values were determined graphically from log concentration inhibition curves (Graphpad Prism 5, GraphPad Software Inc., San Diego, CA, USA). Galanthamine was used as a standard inhibitor.

3.8. Docking Studies

Cocrystal structure of human AChE with compound **1** (PDB code: 4EY7) was obtained from the Protein Data Bank for docking tests (<http://www.rcsb.org>) [26]. The virtual screening was implemented in the Surflex-Dock module of the Sybyl software. Molecules were built with Chemdraw and optimized at molecular mechanical and semiempirical level by using Open Babel GUI. The crystallographic ligand was extracted from the active site and the designed ligands were modelled. All the hydrogen atoms were added to define the correct ionization and tautomeric states, and the carboxylate, phosphonate and sulfonate groups were considered in their charged form. In the docking calculation, the default FlexX scoring function was used for exhaustive searching, solid body optimization, and interaction scoring. Finally, the ligands with the lowest-energy and the most favorable orientation were selected [27].

4. Conclusions

In conclusion, eight meroterpenoids were isolated from the marine derived fungus *Aspergillus versicolor*, including seven new ones, asperversins A–E (**1–7**), and a known one, asperdemin (**8**). Notably, asperversins A (**1**) and B (**2**) possess a unique 5/6/6/6 ring system with a constructed tetrahydrofuran ring. The absolute structures of all new compounds were confirmed by comprehensive

spectroscopic analyses: compound **1** was elucidated by experimental and calculated ECD, and compounds **5** and **7** were ascertained by the X-ray crystallographic diffractions. All isolated meroterpenoids were tested for their acetylcholinesterase enzyme (AChE) inhibitory activities, and compound **7** displayed moderate inhibitory activity against the AChE with an IC₅₀ value of 13.6 μM.

Supplementary Materials: The following are available online at <http://www.mdpi.com/1660-3397/16/5/177/s1>, HRESIMS, 1D and 2D NMR, IR, and UV spectra of **1–7**.

Author Contributions: H.L. conducted the main experiments, data analyzes, and wrote the manuscript; M.D. assisted the isolated experiments; W.S. performed the bioactivity analyzes; C.C. And H.Z. were responsible for the analysis of single-crystal X-ray crystallography. J.W. conducted the fermentation of fungi; C.Q. And Z.L. analyzed the spectroscopic data; J.W., Y.X., and Y.Z. designed the experiments and commented the manuscript. All authors reviewed the manuscript.

Funding: This work was financially supported by the Program for the Changjiang Scholars of Ministry of Education of the People's Republic of China (No. T2016088); the National Science Fund for Distinguished Young Scholars (No. 8172500151); the National Natural Science Foundation of China (Nos. 81573316, 31770379, and 31670354); Innovative Research Groups of the National Natural Science Foundation of China (No. 81721005).

Acknowledgments: We thank the Analytical and Testing Center at Huazhong University of Science and Technology for assistance in testing of ECD, UV, and IR spectra.

Conflicts of Interest: The authors declare no conflict of interest.

References

1. Geris, R.; Simpson, T.J. Meroterpenoids produced by fungi. *Nat. Prod. Rep.* **2009**, *26*, 1063–1094. [[CrossRef](#)] [[PubMed](#)]
2. Matsuda, Y.; Abe, I. Biosynthesis of fungal meroterpenoids. *Nat. Prod. Rep.* **2016**, *33*, 26–53. [[CrossRef](#)] [[PubMed](#)]
3. Morton, R.A. Ubiquinone. *Nature* **1958**, *182*, 1764. [[CrossRef](#)] [[PubMed](#)]
4. Fernholz, E. On the constitution of α -tocopherol. *J. Am. Chem. Soc.* **1938**, *60*, 700–705. [[CrossRef](#)]
5. Moncrief, J.W.; Lipscomb, W.N. Structures of leurocristine (vincristine) and vincalcaleukoblastine. X-ray analysis of leurocristine methiodide. *J. Am. Chem. Soc.* **1965**, *87*, 4963–4964. [[CrossRef](#)] [[PubMed](#)]
6. Kaysser, L.; Bernhardt, P.; Nam, S.J.; Loesgen, S.; Ruby, J.G.; Skewes-Cox, P.; Jensen, P.R.; Fenical, W.; Moore, B.S. Merochlorins A–D, Cyclic Meroterpenoid Antibiotics Biosynthesized in Divergent Pathways with Vanadium-Dependent Chloroperoxidases. *J. Am. Chem. Soc.* **2012**, *134*, 11988–11991. [[CrossRef](#)] [[PubMed](#)]
7. Kaysser, L.; Bernhardt, P.; Nam, S.J.; Loesgen, S.; Ruby, J.G.; Skewes-Cox, P.; Jensen, P.R.; Fenical, W.; Moore, B.S. Correction to “Merochlorins A–D, Cyclic Meroterpenoid Antibiotics Biosynthesized in Divergent Pathways with Vanadium-Dependent Chloroperoxidases”. *J. Am. Chem. Soc.* **2014**, *136*, 14626. [[CrossRef](#)]
8. Awakawa, T.; Zhang, L.H.; Wakimoto, T.; Hoshino, S.; Mori, T.; Ito, T.; Ishikawa, J.; Tanner, M.E.; Abe, I. A Methyltransferase Initiates Terpene Cyclization in Teleocidin B Biosynthesis. *J. Am. Chem. Soc.* **2014**, *136*, 9910–9913. [[CrossRef](#)] [[PubMed](#)]
9. Fischbach, M.A.; Walsh, C.T. Assembly-line enzymology for polyketide and nonribosomal peptide antibiotics: Logic, machinery, and mechanisms. *Chem. Rev.* **2006**, *106*, 3468–3496. [[CrossRef](#)] [[PubMed](#)]
10. Itoh, T.; Tokunaga, K.; Matsuda, Y.; Fujii, I.; Abe, I.; Ebizuka, Y.; Kushiro, T. Reconstitution of a fungal meroterpenoid biosynthesis reveals the involvement of a novel family of terpene cyclases. *Nat. Chem.* **2010**, *2*, 858–864. [[CrossRef](#)] [[PubMed](#)]
11. Macias, F.A.; Varela, R.M.; Simonet, A.M.; Cutler, H.G.; Cutler, S.J.; Dugan, F.M.; Hill, R.A. Novel bioactive breviane spiroditerpenoids from *Penicillium brevicompactum* Dierckx. *J. Org. Chem.* **2000**, *65*, 9039–9046. [[CrossRef](#)] [[PubMed](#)]
12. Zhang, Y.C.; Li, C.; Swenson, D.C.; Gloer, J.B.; Wicklow, D.T.; Dowd, P.F. Novel antiinsectan oxalicine alkaloids from two undescribed fungicolous *Penicillium* spp. *Org. Lett.* **2003**, *5*, 773–776. [[CrossRef](#)] [[PubMed](#)]
13. Guo, C.J.; Knox, B.P.; Chiang, Y.M.; Lo, H.C.; Sanchez, J.F.; Lee, K.H.; Oakley, B.R.; Bruno, K.S.; Wang, C.C.C. Molecular Genetic Characterization of a Cluster in *A. terreus* for Biosynthesis of the Meroterpenoid Terretinin. *Org. Lett.* **2012**, *14*, 5684–5687. [[CrossRef](#)] [[PubMed](#)]

14. Nakamura, H.; Matsuda, Y.; Abe, I. Unique chemistry of non-heme iron enzymes in fungal biosynthetic pathways. *Nat. Prod. Rep.* **2018**. [[CrossRef](#)] [[PubMed](#)]
15. Qi, C.; Bao, J.; Wang, J.; Zhu, H.; Xue, Y.; Wang, X.; Li, H.; Sun, W.; Gao, W.; Lai, Y.; et al. Asperterpenes A and B, two unprecedented meroterpenoids from *Aspergillus terreus* with BACE1 inhibitory activities. *Chem. Sci.* **2016**, *7*, 6563–6572. [[CrossRef](#)] [[PubMed](#)]
16. He, Y.; Hu, Z.; Sun, W.; Li, Q.; Li, X.N.; Zhu, H.; Huang, J.; Liu, J.; Wang, J.; Xue, Y.; et al. Spiroaspertrione A, a Bridged Spirocyclic Meroterpenoid, as a Potent Potentiator of Oxacillin against Methicillin-Resistant *Staphylococcus aureus* from *Aspergillus* sp. T]23. *J. Org. Chem.* **2017**, *82*, 3125–3131. [[CrossRef](#)] [[PubMed](#)]
17. He, Y.; Hu, Z.X.; Li, Q.; Huang, J.F.; Li, X.N.; Zhu, H.C.; Liu, J.J.; Wang, J.P.; Xue, Y.B.; Zhang, Y.H. Bioassay-Guided Isolation of Antibacterial Metabolites from *Emericella* sp. T]29. *J. Nat. Prod.* **2017**, *80*, 2399–2405. [[CrossRef](#)] [[PubMed](#)]
18. Qiao, Y.B.; Zhang, X.T.; He, Y.; Sun, W.G.; Feng, W.Y.; Liu, J.J.; Hu, Z.X.; Xu, Q.Q.; Zhu, H.C.; Zhang, J.W.; et al. Aspermerodione, a novel fungal metabolite with an unusual 2,6-dioxabicyclo[2.2.1] heptane skeleton, as an inhibitor of penicillin-binding protein 2a. *Sci. Rep.* **2018**, *8*, 5454. [[CrossRef](#)] [[PubMed](#)]
19. Zhou, P.; Wu, Z.; Tan, D.; Yang, J.; Zhou, Q.; Zeng, F.; Zhang, M.; Bie, Q.; Chen, C.; Xue, Y.; et al. Atrichodermones A–C, three new secondary metabolites from the solid culture of an endophytic fungal strain, *Trichoderma atroviride*. *Fitoterapia* **2017**, *123*, 18–22. [[CrossRef](#)] [[PubMed](#)]
20. Yurchenko, A.N.; Smetanina, O.F.; Kalinovskiy, A.I.; Pivkin, M.V.; Dmitrenok, P.S.; Kuznetsova, T.A. A new meroterpenoid from the marine fungus *Aspergillus versicolor* (Vuill.) Tirab. *Russ. Chem. Bull.* **2010**, *59*, 852–856. [[CrossRef](#)]
21. Wang, J.F.; Wei, X.Y.; Qin, X.C.; Tian, X.P.; Liao, L.; Li, K.M.; Zhou, X.F.; Yang, X.W.; Wang, F.Z.; Zhang, T.Y.; et al. Antiviral Merosesquiterpenoids Produced by the Antarctic Fungus *Aspergillus ochraceopetaliformis* SCSIO 05702. *J. Nat. Prod.* **2016**, *79*, 59–65. [[CrossRef](#)] [[PubMed](#)]
22. Kaur, A.; Raja, H.A.; Swenson, D.C.; Agarwal, R.; Deep, G.; Falkinham, J.O.; Oberlies, N.H. Talarolutins A–D: Meroterpenoids from an endophytic fungal isolate of *Talaromyces minioluteus*. *Phytochemistry* **2016**, *126*, 4–10. [[CrossRef](#)] [[PubMed](#)]
23. Zhan, G.Q.; Liu, J.J.; Zhou, J.F.; Sun, B.; Aisa, H.A.; Yao, G.M. Amaryllidaceae alkaloids with new framework types from *Zephyranthes candida* as potent acetylcholinesterase inhibitors. *Eur. J. Med. Chem.* **2017**, *127*, 771–780. [[CrossRef](#)] [[PubMed](#)]
24. Chen, S.H.; Chen, D.N.; Cai, R.L.; Cui, H.; Long, Y.H.; Lu, Y.J.; Li, C.Y.; She, Z.G. Cytotoxic and Antibacterial Preussomerins from the Mangrove Endophytic Fungus *Lasiodiplodia theobromae* ZJ-HQ1. *J. Nat. Prod.* **2016**, *79*, 2397–2402. [[CrossRef](#)] [[PubMed](#)]
25. Ellman, G.L.; Courtney, K.D.; Andres, V., Jr.; Feather-Stone, R.M. A new and rapid colorimetric determination of acetylcholinesterase activity. *Biochem. Pharmacol.* **1961**, *7*, 88–95. [[CrossRef](#)]
26. Cheung, J.; Rudolph, M.J.; Burshteyn, F.; Cassidy, M.S.; Gary, E.N.; Love, J.; Franklin, M.C.; Height, J.J. Structures of Human Acetylcholinesterase in Complex with Pharmacologically Important Ligands. *J. Med. Chem.* **2012**, *55*, 10282–10286. [[CrossRef](#)] [[PubMed](#)]
27. Feng, X.; Ambia, J.; Chen, K.M.; Young, M.; Barth, P. Computational design of ligand-binding membrane receptors with high selectivity. *Nat. Chem. Biol.* **2017**, *13*, 715–723. [[CrossRef](#)] [[PubMed](#)]

